THE JOURNAL OF BIOLOGICAL CHEMISTRY
Vol. 275, No. 35, Issue of September 1, pp. 27238–27244, 2000
© 2000 by The American Society for Biochemistry and Molecular Biology, Inc.
Printed in U.S.A.

Crystal Structure of Human Parathyroid Hormone 1–34 at 0.9-Å Resolution*

Received for publication, February 10, 2000, and in revised form, May 26, 2000
Published, JBC Papers in Press, June 2, 2000, DOI 10.1074/jbc.M001134200

Lei Jin, Stephen L. Briggs, Srinivasan Chandrasekhar, Nickolay Y. Chirgadze, David K. Clawson, Richard W. Schevitz, David L. Smiley, Armen H. Tashjian, and Faming Zhang‡

From the Lilly Research Laboratories, Eli Lilly & Company, Indianapolis, Indiana 46285

The N-terminal fragment 1–34 of parathyroid hormone (PTH), administered intermittently, results in increased bone formation in patients with osteoporosis. PTH and a related molecule, parathyroid hormone-related peptide (PTHrP), act on cells via a common PTH/PTHrP receptor. To define more precisely the ligand-receptor interactions, we have crystallized human PTH (hPTH)-(1–34) and determined the structure to 0.9-Å resolution. hPTH-(1–34) crystallizes as a slightly bent, long helical dimer. Analysis reveals that the extended helical conformation of hPTH-(1–34) is the likely bioactive conformation. We have developed molecular models for the interaction of hPTH-(1–34) and hPTHrP-(1–34) with the PTH/PTHrP receptor. A receptor binding pocket for the N terminus of hPTH-(1–34) and a hydrophobic interface with the receptor for the C terminus of hPTH-(1–34) are proposed.

Parathyroid hormone (PTH)[1] is an 84-amino acid polypeptide that regulates extracellular calcium homeostasis via actions directly on kidney and bone and indirectly on intestine by facilitating calcium absorption (1). Subcutaneous administration of hPTH-(1–34) once a day stimulates bone formation and increases bone mass in patients with osteoporosis (2) and ovariectomized monkeys (3). Thus, hPTH-(1–34) has potential medical and pharmaceutical applications to the treatment of osteoporosis (4).

PTH has both anabolic and catabolic effects on the skeleton. Persistent elevation of PTH causes increased bone resorption, whereas intermittently administered PTH results in enhanced bone formation (5). The mechanism by which PTH exhibits its dual effects is not known. PTH interacts with a G protein-coupled, seven-transmembrane helix receptor (PTH/PTHrP or PTH1 receptor) to stimulate adenylyl cyclase (6) and phospholipase C (7) activities. Studies, both *in vitro* and *in vivo*, have shown that the N-terminal 1–34 fragment has the same biological activities as the intact hormone in eliciting cAMP responses and in stimulating bone formation (8). Truncation and mutagenesis studies on PTH-(1–34) have revealed that the N-terminal region is critical for activation of receptor signaling, whereas the N-terminal truncated peptide PTH-(3–34) is only a partial agonist, and the further shortened peptide PTH-(7–34) becomes a low affinity antagonist (9, 10). Residues 17–31, near the C terminus of PTH-(1–34), are required for high affinity receptor binding (11).

PTHrP is a polypeptide that is over-expressed in certain tumors and causes the syndrome of malignancy-associated humoral hypercalcemia (12). Under physiological conditions, PTHrP is produced locally in a wide variety of tissues and is involved in cell growth, differentiation, and development of the fetal skeleton. There are 6 identical amino acids in the first 13 amino acids in the known PTH and PTHrP sequences (Fig. 1). Like PTH, PTHrP binds to the same G protein-coupled receptor, and its N-terminal fragment PTHrP-(1–34) has many functions that mimic those of full-length PTHrP-(1–141) as well as PTH-(1–34) and full-length PTH-(1–84) (12, 13). In addition, hPTH-(1–34) and hPTHrP-(1–34) have similar three-dimensional structures based on NMR studies (14, 15).

Various methods have been used to determine the structure of PTH, including dark-field electron microscopy, fluorescence spectroscopy, circular dichroism, and nuclear magnetic resonance (NMR) spectroscopy (14–23). Results from these diverse approaches have not yet yielded a consistent structure for this peptide. In part, this uncertainty arises from the flexible nature of small peptides in solution as well as from different experimental conditions such as protein concentration, solvent conditions, pH, temperature, and different methods used for data interpretation. The general consensus is that PTH-(1–34) and PTHrP-(1–34) have an N-terminal helix and a C-terminal helix that vary in length and stability depending on the specific experimental conditions and are connected by a highly flexible mid-region. The C-terminal helix is more stable than the N-terminal helix. In aqueous solution, PTH-(1–34) and PTHrP-(1–34) form fewer and less stable secondary structural elements than under membrane-mimicking conditions, such as dodecylphosphocholine micelles (20) or palmitoyloleoylphosphatidylserine vesicles (23), or in the presence of a secondary structure-inducing solvent such as trifluoroethanol (TFE) (18–20, 22, 23). Several of the NMR studies have been interpreted to show a "U-shaped" tertiary structure with the N- and C-terminal helices interacting with each other to form a hydrophobic core (17, 18). However, the majority of the NMR analyses of PTH and PTHrP do not provide evidence of long range interactions between the two helices. To create more potent and orally available analogs of PTH, detailed structural information on the peptide should aid in characterizing the molecular interactions between the ligand and receptor.

* The costs of publication of this article were defrayed in part by the payment of page charges. This article must therefore be hereby marked "*advertisement*" in accordance with 18 U.S.C. Section 1734 solely to indicate this fact.

The atomic coordinates and structure factors (codes 1ET1, 1ET2, and 1ET3) have been deposited in the Protein Data Bank, Research Collaboratory for Structural Bioinformatics, Rutgers University, New Brunswick, NJ (http://www.rcsb.org/).

‡ To whom correspondence should be addressed: Lilly Research Laboratories, Lilly Corporate Center, Drop Code 0403, Eli Lilly & Company, Indianapolis, IN 46285. Tel.: 317-277-6110; Fax: 317-276-9722; E-mail: zfm@lilly.com.

[1] The abbreviations used are: PTH, parathyroid hormone; hPTH, human PTH; PTHrP, parathyroid hormone-related peptide; TFE, trifluoroethanol; TM, transmembrane.

This paper is available on line at http://www.jbc.org

Downloaded from http://www.jbc.org/ by guest on November 12, 2017

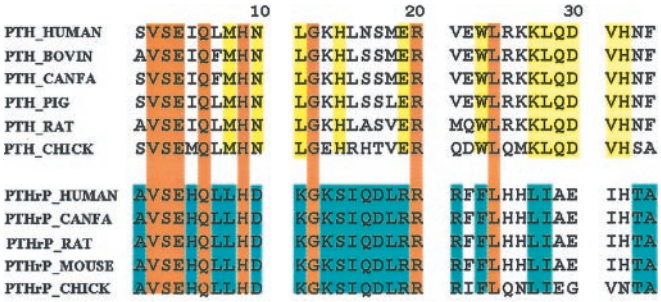

FIG. 1. **Sequence alignment of known species of PTH-(1–34) and PTHrP-(1–34).** The invariant residues are *shaded* in *orange*. The conserved residues in PTH-(1–34) are *shaded* in *yellow*, whereas the conserved residues in PTHrP-(1–34) are in *blue*. BOVIN, bovine; CANFA, *canis familiaris* (dog).

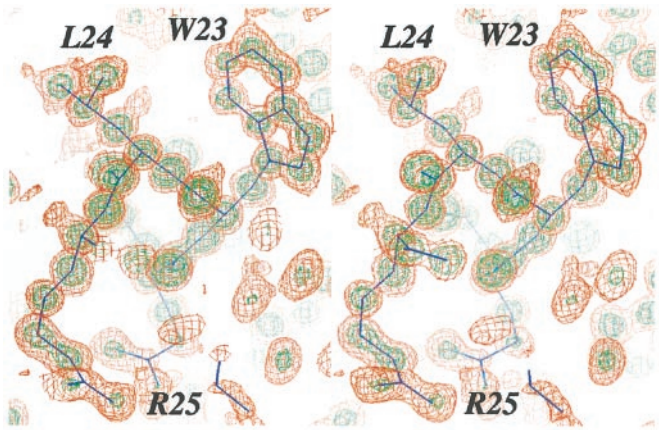

FIG. 2. **Stereo diagram of the $2F_o$-F_c electron density map covering residues Trp[23], Leu[24], and Arg[25] and several water molecules.** The map was calculated using the native data including all reflections from 14 to 0.9 Å. The map in *orange* is contoured at 1.0σ, and the map in *green* is contoured at 3.5σ.

EXPERIMENTAL PROCEDURES

Peptide Purification—Human PTH-(1–34) (LY333334, Lilly) was expressed in *Escherichia coli* cells. The inclusion bodies were solubilized in 7 M urea and captured by a reverse phase column. hPTH-(1–34) was purified through a cation exchange-column (FFSP, Amersham Pharmacia Biotech) with a gradient of 0.1–0.3 M sodium chloride at pH 2.5 in 7 M urea followed by a reverse phase column with a gradient of 22–32% acetonitrile in 20 mM glycine at pH 9, refolded, and freeze-dried. Selenomethionine hPTH-(1–34) was synthesized on an ABI-430A peptide synthesizer using *t*-butoxycarbonyl amino acids. The *t*-butoxycarbonyl seleno-L-methionine was prepared from L-selenomethionine using di-*t*-butyldicarbonate. The selenomethionine hPTH-(1–34) was purified by a Vydac C18 column with a gradient of 10–50% acetonitrile in 0.1% trifluoroacetic acid at pH 2 and Phenomenex Primeshere 10 C18 column with a gradient of 15–35% acetonitrile in 0.05 M ammonium bicarbonate at pH 8 on a fast protein liquid chromatography system (Amersham Pharmacia Biotech). Identified fractions were pooled, frozen, and lyophilized. Mass spectroscopy analysis showed complete incorporation of selenomethionine into the peptide.

Crystallization and Data Collection—hPTH-(1–34) was crystallized at 20 °C by the hanging drop vapor diffusion method. Single crystals were obtained by mixing 20 mg ml^{-1} hPTH-(1–34) in 20% glycerol, at a 1:1 ratio (v/v), with a solution containing 2.5 M ammonium sulfate, 5% isopropanol, and 0.1 M sodium acetate buffer, pH 4.5. Crystals appeared overnight and continuously grew to 0.6 × 0.2 × 0.1 mm^3 in a week. Crystals of selenomethionine hPTH-(1–34) were obtained by repeated seeding under the same conditions as described above with 10 mg ml^{-1} selenomethionine hPTH-(1–34) in 20% glycerol and 20 mM sodium citrate, pH 4.5.

For cryogenic data collection, hPTH-(1–34) crystals were flash-frozen in liquid nitrogen. X-ray data were collected at −170 °C by a Mar CCD detector at the Industrial Macromolecule Crystallography Association beam line ID-17 at Advanced Photon Source in Argonne National Laboratories. Data were integrated and reduced using the program HKL2000 (24). The crystals belong to hexagonal space group $P6_5$ with unit cell dimensions of 30.18 Å (a) and 110.44 Å (c). Three data sets were collected for a selenomethionine hPTH-(1–34) crystal at wavelengths of 0.9795, 0.97936, and 0.9840 Å for multiple wavelength anomalous dispersion phasing (see Table I).

Structure Determination—The structure was solved by the program SOLVE (25) with the multiple wavelength anomalous dispersion data. The polypeptide chain was fitted to the electron density with program O (26). The model was refined to 2.0-Å resolution using the multiple wavelength anomalous dispersion data and to 0.9-Å resolution using the native data in X-PLOR98 (27) by simulated annealing. The model was then further refined in SHELX 97 (28) by the conjugate gradient algorithm with riding hydrogens. Six-parameter anisotropic temperature factors for all non-H atoms were included, and after anisotropic refinement, the *R* factor fell from 20 to 14%, and R_{free} fell from 22 to 17%. Sequential model building processes were carried out in QUANTA (Molecular Simulations, Inc.) against $2F_o - F_c$ and $F_o - F_c$ maps. The final *R* factor for all data is 13.7%; R_{free} is 14%. The final structure contains 660 non-hydrogen protein atoms and 104 water molecules. All residues are in the most favorable conformation in Ramachandran plot.

Molecular Modeling—Molecular modeling was carried out in QUANTA using the protein design tools. The seven transmembrane domains of the PTH/PTHrP receptor were first determined by several programs for transmembrane region detection provided by the ExPASy Molecular Biology Server, and then a consensus alignment was determined. The crystal structure of bacteriorhodopsin at 1.9 Å (PDB code 1QHJ, Ref. 29) was used as a template for the topological orientation and arrangement of the transmembrane (TM) helices. Sequences of the transmembrane helices for the PTH/PTHrP receptor and bacteriorhodopsin were aligned, and then homology modeling was carried out to create the TM helices of the PTH/PTHrP receptor. The conformations of the intracellular and extracellular loops were constructed in QUANTA using the fragment data base-searching algorithm. For the N-terminal receptor region 168–198, the NMR structure determined in a lipid environment (30) (PDB code 1BL1) was incorporated into the model. This was accomplished by aligning the membrane-embedded helix (residues 190–196) with the beginning of TM1. The final model of the receptor contains residues 168–469 of the whole length, residues 1–593.

One hPTH-(1–34) monomer, derived from the crystal structure, was docked into the receptor using two constraints based on cross-linking studies (31, 32). Energy minimization was applied to the complex of hPTH-(1–34) and residues 168–198 of the receptor using the default setting in QUANTA until no significant changes were observed. The hPTHrP-(1–34) model was produced by homology modeling using the crystal structure of hPTH-(1–34) as a template. The model of hPTHrP-(1–34) binding to the PTH/PTHrP receptor was created similarly to the hPTH-(1–34)-receptor complex.

RESULTS AND DISCUSSION

Overall Structure—The structure of hPTH-(1–34) was determined by the multiple wavelength anomalous dispersion method using selenomethionine hPTH-(1–34) with the program SOLVE (25). The structure was then refined anisotropically to a resolution of 0.9 Å against a native data set with the program SHELX97 (28) (Fig. 2, Table I). Inclusion of anisotropic motion for the *B* factor refinement decreased the *R* factor significantly. The overall structure of hPTH-(1–34) is a slightly bent helix (Fig. 3*a*). The bend is located between residues 12 and 21 with a bending angle of 15° between the N-terminal helix (residues 3–11) and the C-terminal helix (residues 21–33). Hydrogen bonds between the side chains of Asn^{16} and Glu^{19}, Ser^{17} and Arg^{20}, and a salt bridge between Glu^{22} and Arg^{25} are observed (Fig. 3*a*). Although hPTH-(1–34) is a continuous helix, residues 6–20 and residues 21–33 form two amphiphilic helices, with the hydrophobic sides of these helices facing in different directions. Thus, the hydrophobic residues of hPTH-(1–34) form a twisted belt from the N terminus to the C terminus with the crossing point near residue Arg^{20} (Fig. 3*a*). Gly^{12} is a conserved residue in all the known PTH and PTHrP species (Fig. 1). Despite the flexible nature of glycine, Gly^{12} is in a strict helical conformation in the crystal structure. Substitution of Gly^{12} with Ala, a helix promotor, in [Tyr^{34}]hPTH-(1–34)NH_2 was well tolerated, whereas substitution with Pro, a

Downloaded from http://www.jbc.org/ by guest on November 12, 2017

TABLE I
Data collection, phasing, and refinement statistics

Diffraction data (space group $P6_5$)				
	Native data	MAD data		
		Peak	Inflection point	Remote point
Wavelength (Å)	1.00000	0.97936	0.97950	0.98400
Unit cell dimensions				
a (Å)	30.18	30.19	30.14	30.16
c (Å)	110.44	111.04	110.88	110.96
Resolution range	14.0–0.9	20.0–2.0	20.0–2.0	20.0–2.0
Total reflections	111749	41976	38623	43184
Unique reflections	37765	3894	3859	3865
Completeness (%)[a]	90.5 (75.5)	99.7 (99.5)	99.7 (99.5)	99.7 (99.5)
R_{merge}[b] (%)[a]	5.4 (16.3)	6.1 (11.1)	6.1 (11.6)	5.1 (8.9)
Phasing by SOLVE (20.0–2.0 Å)				
Mean figure of merit				0.86
Refinement statistics (15.0–0.9 Å)				
		$F_o > 0\sigma$		$F_o > 4\sigma$
R_{work}[c] (%)		13.7		12.7
R_{free}[c] (%)		14.0		13.0
Final model				
		Atoms (protein/solvent)		Average *B* (main chain/side chain)
RMS deviation from ideality Bond length (Å), 0.015 Bond angles (°), 2.259 Dihedral angles (°), 16.628		660/104		7.05/11.74Å^2

[a] The numbers in the parentheses are statistics for the highest resolution shell.
[b] $R_{merge} = \Sigma|I_i - \langle I\rangle|/\Sigma\ I_i$, where I_i is the intensity of an individual measurement, and $\langle I\rangle$ is the mean intensity of all measurements of I.
[c] $R = \Sigma||F_o| - |F_c||/\Sigma|F_o|$. R_{work} is calculated using 95% of the reflections, whereas R_{free} is calculated using 5% of the reflections.

helix breaker, decreased receptor binding affinity 840-fold and adenylyl cyclase-stimulating activity 3500-fold (33). Together, these findings indicate that the helical conformation around Gly^{12} is essential for full biological activity.

hPTH-(1–34) crystallizes as a dimer in the hexagonal space group $P6_5$. His^{14} and Ser^{17} from both molecules are located at the crossing point of the X-shaped dimer (Fig. 3, *b* and *c*). The N_δ of His^{14} from one molecule forms a hydrogen bond with N_δ of His^{14} from another molecule, whereas Ser^{17} from one molecule packs against the imidazole ring of His^{14} from the other molecule (Fig. 3, *b* and *c*). Within the dimer interface, hydrophobic interactions extend from the crossing point toward the N and C termini. Residues Leu^7, Leu^{11}, and Leu^{15} of the N-terminal amphiphilic helix from one molecule are in van der Waals contact with residues Leu^{24}, Val^{21}, and Met^{18} of the C-terminal amphiphilic helix from the other molecule.

The main chain conformation of each molecule in the dimer is quite similar except for the conformation of the N-terminal residue Ser^1 that deviates somewhat from its counterpart. Thus, the root mean square deviation is 0.05 Å when the main chain atoms of residues 2–34 from two molecules are superimposed and 0.09 Å when all main chain atoms of residues 1–34 are used. The side chains of several residues adopt different conformations in the different monomers. Three alternative conformations for Ser^{17} and Glu^{22} and two alternative conformations for Ser^3, Leu^7, His^{14}, Met^{18}, and His^{32} are observed in each molecule. Residues Ile^5 and Met^8 have one conformation in one molecule and two in the other. The side chain conformations of residues Gln^6, Lys^{26}, and Lys^{27} are not superimposable between the two molecules. Because of these different conformations and different water structures around the monomers, hPTH-(1–34) crystallizes as a dimer in the asymmetric unit in the space group $P6_5$ rather than as a monomer in the higher symmetry space group $P6_522$. Our results from ultracentrifugation studies with hPTH-(1–34), in a solution that was close to crystallization conditions, did not demonstrate stable dimer formation, which is consistent with previous ultracentrifugation results obtained from hPTH-(1–37) (17). Thus, the dimer seen here is most likely a lattice effect in crystal packing rather than an intrinsic property of PTH-(1–34) in solution.

Comparison of the Crystal Structure with NMR Structures—Extensive NMR studies have been carried out on PTH and PTHrP in different solvent environments (14). In general, NMR studies show that PTH-(1–34) and PTHrP-(1–34) form an N-terminal helix and a C-terminal helix connected by a highly flexible region in solution. Fig. 4 shows the superposition of the crystal structure with the NMR structure of hPTH-(1–34) with PDB code 1HPY (34) by superimposing the Cα atoms of the C-terminal helices (residues 18–28). Superposition of the crystal structure with other NMR structures, such as hPTH-(1–37) (PDB code 1HPH) (17) and hPTHrP-(1–34) (PDB code 1BZG) (15) yielded similar pictures as Fig. 4 (not shown). These NMR structures were obtained under near physiological conditions. The highly flexible region in the NMR structures (residues 10–20) is found to form a regular helix in our crystal structure. Evidence from several NMR studies on PTH-(1–34) and PTHrP-(1–34) leads to the conclusion that the helical content increases with increasing TFE concentration or conditions that mimic the membrane environment. In 70% TFE, the N- and C-terminal helices (residues 3–13 and 15–29, respectively) of PTH-(1–34) were very regular, with a short discontinuity at residue 14 (35). NMR structures of PTHrP-(1–34) in 50% TFE also showed two well defined helices (residues 3–12 and 17–33) (14). Our crystal structure is similar to the NMR structures determined in high concentrations of TFE or under membrane-mimicking conditions (14, 35). This similarity is not surprising because hPTH-(1–34) in the crystal has very limited solvent exposure. The solvent content of the hPTH-(1–34) crystal is less

Downloaded from http://www.jbc.org/ by guest on November 12, 2017

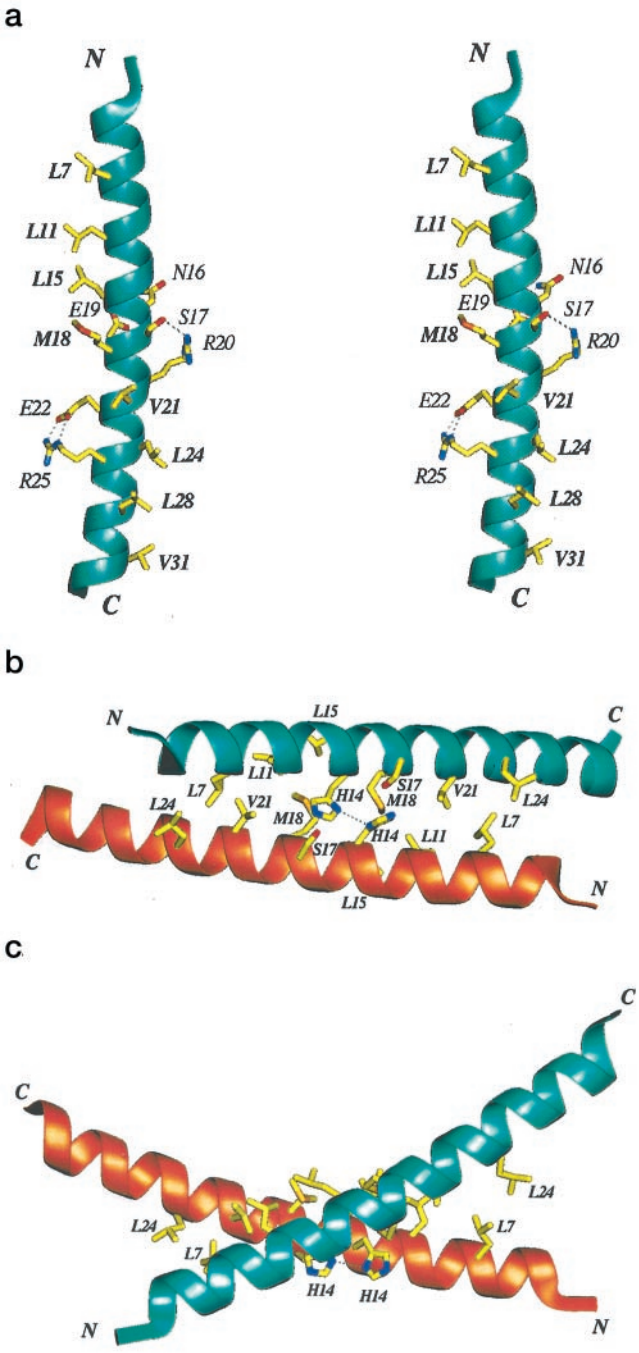

FIG. 3. **Overall structure of hPTH-(1–34).** *a*, hPTH-(1–34) monomer is a slightly bent helix presented as a *blue ribbon* in stereo view. Residues 6–20 and 21–33 form two amphiphilic helices with their hydrophobic side chains facing in different directions. The nonpolar residues of the amphiphilic helices (Leu[7], Leu[11], Leu[15], Met[18], Val[21], Leu[24], Leu[28], and Val[31]) are shown. The crossing point of the two amphiphilic helices is located close to Arg[20]. Hydrogen bonds and salt bridges are shown as *dotted lines* between Asn[16] and Glu[19], Ser[17] and Arg[20], and Glu[22] and Arg[25]. *b*, hPTH-(1–34) dimer is presented as *blue* and *orange ribbons*, and the residues forming the dimer interface are *highlighted*. The dimer interface is mainly hydrophobic. At the crossing point of the X-shaped dimer, the His[14] from each chain form a hydrogen bond shown as a *dotted line*, and Ser[17] from one molecule packs against the imidazole ring of His[14] from another molecule. *c*, the hPTH-(1–34) dimer in a view rotated 90° forward around the *x* axis from *b*.

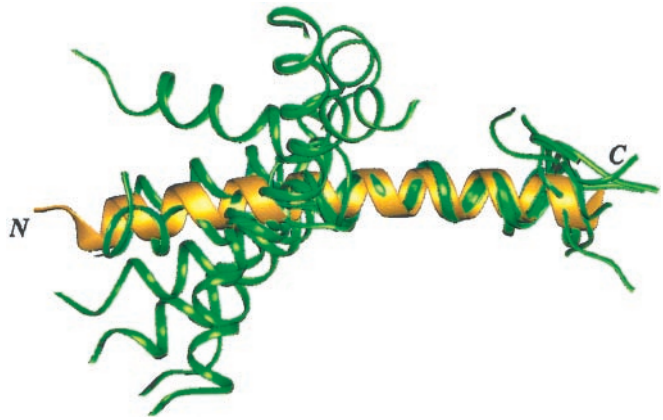

FIG. 4. **Superposition of the crystal structure of hPTH-(1–34) with NMR structures of hPTH-(1–34) with PDB code 1HPY.** The Cα atoms of the C-terminal helix (18–28) were superimposed. The crystal structure of hPTH-(1–34) (in *gold*) is presented as a *thick ribbon*; NMR structures are presented as *thin ribbons* (in *green*). The crystal structure of hPTH-(1–34) is in extended helical conformation, which is different from the NMR structures that possess N- and C-terminal helices connected by a flexible loop.

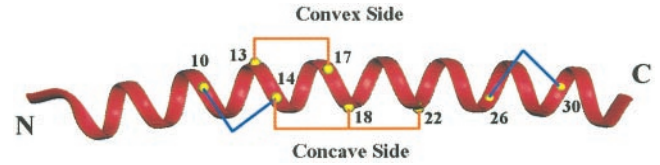

FIG. 5. **Positions of lactam bridges introduced in hPTH-(1–31) and hPTHrP-(1–34).** hPTH-(1–34) is presented as a *red ribbon*. The Cα atoms of the residues that were connected by lactam bridges are shown as *yellow balls*. The lactam bridges (between residues 13 and 17, 14 and 18, and 18 and 22) that increased the biological activity are connected by *orange lines*. They are located in the mid-region of the molecule and on either the convex or concave sides of the helical arc. The lactam bridges (between residues 10 and 14 and 26 and 30) that significantly decreased the biological activity are connected by *blue lines* and are located on the sides of the helical arc.

than 30%, with extensive hydrophobic protein-protein interactions. In fact, the crystal structure might represent the conformation of PTH-(1–34) when it is close to its membrane receptor as proposed for the NMR structures under high concentrations of TFE or membrane-mimicking conditions (23).

Bioactive Conformations of PTH-(1–34) and PTHrP-(1–34)—Previous studies that have involved searching for the bioactive conformations of PTH and PTHrP have used lactam cyclizations designed to stabilize secondary structural elements to probe for the presence of these conformations. Lactam bridges were introduced at different locations along the peptide to connect the side chains at i and $i + 4$ positions in an effort to stabilize a helical conformation. Structural and functional studies have suggested that increasing helical content by such conformational constraints may increase biological potency, but this result is highly sensitive to the constrained positions. Condon *et al.* (42) reported that adenylyl cyclase-stimulating activity in ROS 17/2.8 cells was increased when a lactam bridge was introduced between residues 14 and 18 or 18 and 22 of hPTH-(1–31) but decreased when the lactam bridge was introduced between residues 10 and 14. In PTHrP, when lactamization was introduced between residues 13 and 17, adenylyl cyclase-stimulating activity was also increased (36). However, a lactam bridge introduced between residues 26 and 30 resulted in 400 times lower binding affinity and 30 times lower adenylyl cyclase-stimulating activity (36).

Interestingly, the lactam-containing structures of hPTH-(1–31) (42) and hPTHrP-(1–34) (36) were both in extended helical conformations, very similar to our crystal structure of hPTH-(1–34). In the crystal structure of hPTH-(1–34), the three well tolerated lactam bridges (residues 13–17, 14–18, and 18–22) are located on either the convex or concave sides of the arc

Downloaded from http://www.jbc.org/ by guest on November 12, 2017

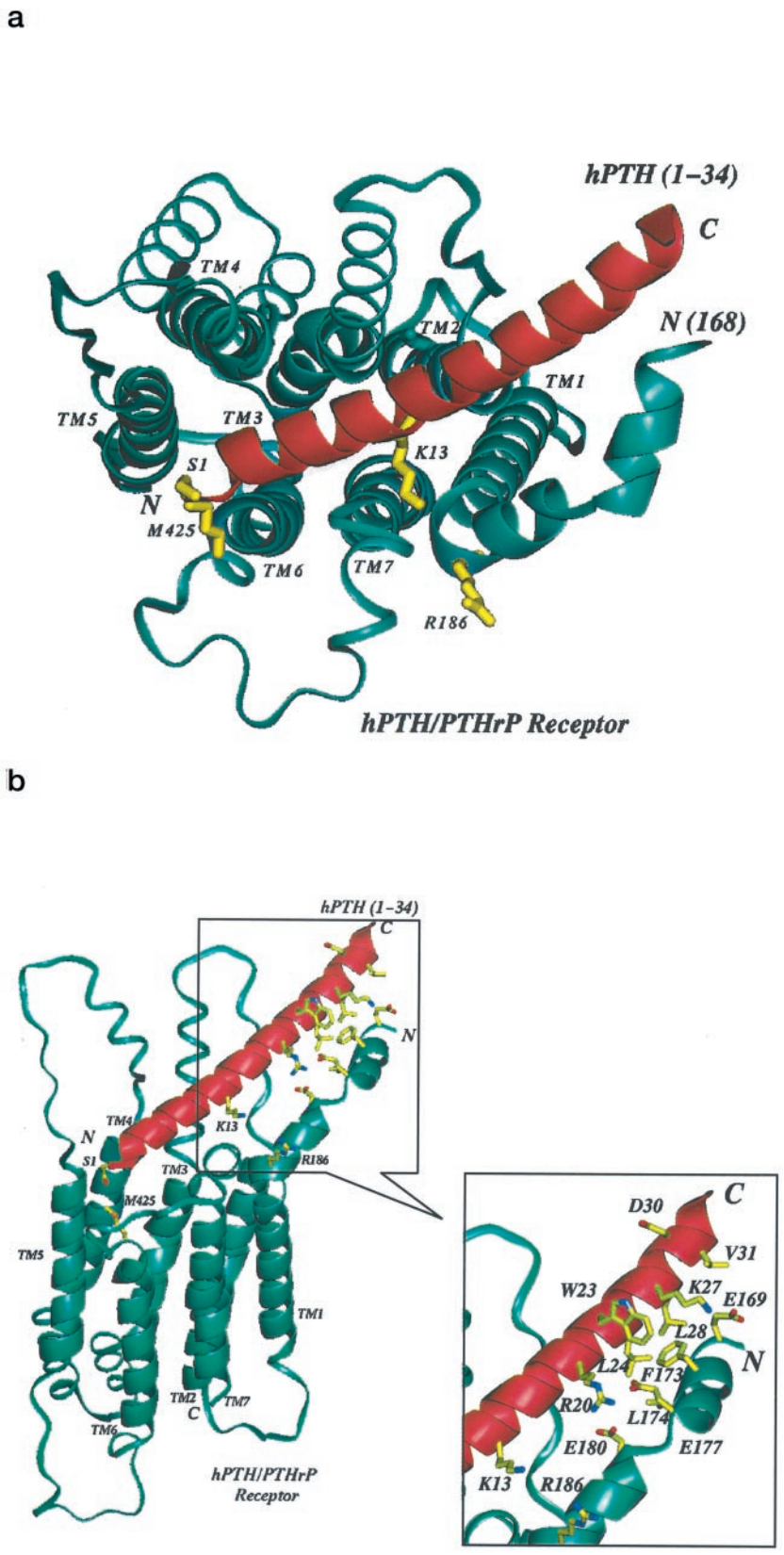

FIG. 6. **Model of hPTH-(1–34) binding to the PTH/PTHrP receptor.** The crystal structure of hPTH-(1–34) is in *red*, and the receptor is in *blue*. Residues at the ligand-receptor interface are highlighted in *yellow*. *a*, a top view of the model looking down the seven transmembrane helices. Residues Ser^{1} and Lys^{13} of hPTH-(1–34) and Met^{425} and Arg^{186} of the receptor are shown, which were used to dock hPTH-(1–34) to the receptor. *b*, a side view of the model rotated 90 ° from the view in *a*. Residues forming the interface between the C terminus of hPTH-(1–34) and the receptor are *highlighted*. A hydrophobic patch is formed by residues Trp^{23}, Leu^{24}, and Leu^{28} of hPTH-(1–34) and Phe^{173} and Leu^{174} of the receptor. Arg^{20} of hPTH-(1–34) interacts with Glu^{177} and Glu^{180} of the receptor, whereas Lys^{27} of hPTH-(1–34) interacts with Glu^{169} of the receptor.

formed by the slightly bent helix and are in the mid-region of the molecule (Fig. 5). Thus, it appears that enhancing helical structure in this flexible region of the peptide increases the biological activity of PTH and PTHrP. The poorly tolerated bridges (residues 10–14 and 26–30) are located on the sides of the hPTH-(1–34) helical arc (Fig. 5). In these cases, the decreased biological activities may be caused by twisting the helical arc sideways or interfering with the ligand-receptor interaction when lactam bridges were introduced at those positions. Thus, rigidity in the middle region of hPTH-(1–34) as well as the bending direction of the helix appears to have significant functional effects. Therefore, the extended helical conformation observed in the crystal structure may well represent the active receptor binding conformation of hPTH-(1–34).

Downloaded from http://www.jbc.org/ by guest on November 12, 2017

hPTH-(1–34) could be in a flexible conformation in solution as would occur in the extracellular space, but a regularized helical conformation is likely to be induced when the peptide approaches the hydrophobic membrane before receptor binding. These hypotheses are examined further by the following molecular modeling results.

Model of hPTH-(1–34) Binding to the PTH/PTHrP Receptor—Previous studies on PTH- or PTHrP-receptor interactions have suggested that the juxtamembrane region of the TM helices and extracellular loops (especially the third loop) of the PTH/PTHrP receptor interact with the N terminus of PTH or PTHrP agonists to induce second messenger signaling (37); the N-terminal extracellular region of the receptor interacts with the C-terminal region (residues 15–34) of either PTH or PTHrP during ligand binding (11). Results from photoaffinity cross-linking by *p*-benzoylphenylalanine and site-directed mutagenesis identified two contact points in the PTH-(1–34)·PTH/PTHrP receptor complex, Ser^{1} of hPTH-(1–34) to Met^{425} of the receptor (31) and Lys^{13} of hPTH-(1–34) to Arg^{186} of the receptor (32). A model of the hPTH-(1–34) bound to the PTH/PTHrP receptor was created by incorporating these restraints. Our model of the PTH/PTHrP receptor was generated by homology modeling using the 1.9-Å resolution crystal structure of bacteriorhodopsin (PDB code 1QHJ) (29) as a template for the seven transmembrane helices. The conformations of the intracellular and extracellular loops were constructed by a fragment data base-searching algorithm. The NMR structure of the putative ligand-binding domain of the receptor (30), residues 168–196, was also incorporated. hPTH-(1–34) was docked to the receptor utilizing the previous knowledge of the ligand-receptor interactions identified by photoaffinity cross-linking and site-directed mutation studies (31, 32).

In our model (Fig. 6*a*) the N-terminal region of hPTH-(1–34), responsible for its agonist activity, binds to a pocket consisting of the extracellular portion of TM3, TM4, and TM6 and the second and third extracellular loops of the receptor. The middle region of hPTH-(1–34) is sandwiched between the first extracellular loop and the N-terminal extracellular region of the receptor adjacent to TM1. The C-terminal region of hPTH-(1–34) forms extensive interactions with the putative binding domain of the PTH/PTHrP receptor (Fig. 6*b*). This interface consists of the hydrophobic interactions (residues Leu^{24}, Trp^{23}, and Leu^{28} of hPTH-(1–34) and Phe^{173} and Leu^{174} of the receptor) and hydrophilic interactions between Arg^{20} of hPTH-(1–34) and Glu^{180} and Glu^{177} of the receptor as well as between Lys^{27} of hPTH-(1–34) and Glu^{169} of the receptor.

Several models utilizing the NMR structure of hPTH-(1–34) with N- and C-terminal helices connected by a flexible loop have been proposed in the literature for the binding of hPTH-(1–34) to the PTH/PTHrP receptor. Bisello *et al.* (31) have suggested that the N terminus of hPTH-(1–34) locates close to the extracellular end of TM6. In a recent model, the N-terminal helix of PTH locates within a space surrounded by the extracellular portion of the seven transmembrane helices and extracellular loops, whereas the C-terminal helix of hPTH-(1–34) has two possible orientations relative to the N-terminal extracellular region of the receptor (38). Using the crystal structure of hPTH-(1–34) with its extended helical conformation, only one orientation of hPTH-(1–34) in our model satisfies all the known ligand-receptor contact restraints (Fig. 6*b*).

Site-directed mutagenesis studies in the C-terminal region of hPTH-(1–34) have suggested that Leu^{24} and Leu^{28} are intolerant to mutation (39). When Leu^{24} and Leu^{28} are substituted by Glu, the receptor binding affinities decrease 4000- and 1600-fold, respectively. A less dramatic reduction of receptor binding affinity (40-fold) is observed when Val^{31} is replaced by Glu. In contrast, replacement of Asp^{30} by Lys has no effect on receptor binding. In our model (Fig. 6*b*), Leu^{24} and Leu^{28} of hPTH-(1–34) are located at the center of the hydrophobic interface, whereas Val^{31} is located at the end of the hydrophobic patch. Asp^{30} is exposed to solvent; therefore, the lysine mutant at this position would not change receptor binding affinity. The hydrophilic interaction between Lys^{27} of hPTH-(1–34) and Glu^{169} of the PTH/PTHrP receptor may be less important for binding than other interactions because a variety of mutations were tolerated at Lys^{27} (39). To confirm this model, additional site-directed mutagenesis studies must be carried out on residues at the interface discussed above.

Model of hPTHrP-(1–34) Binding to the PTH/PTHrP Receptor—It has been proposed that PTHrP-(1–34) binds to the PTH/PTHrP receptor in the same fashion as does PTH-(1–34) (38). We have constructed a homology model of hPTHrP-(1–34) using the crystal structure of hPTH-(1–34) and docked hPTHrP-(1–34) to the PTH/PTHrP receptor with the same orientation as hPTH-(1–34). This was followed by energy minimization. Residues Arg^{20} and Leu^{24} are conserved among all the known PTH and PTHrP sequences, whereas residues 23, 28, and 31 are all hydrophobic residues that are functionally conserved (Fig. 1). Residues Arg^{20}, Phe^{23}, Leu^{24}, Ile^{28}, and Ile^{31} of hPTHrP-(1–34) form similar interactions with receptor (not shown) as the corresponding residues of hPTH-(1–34) in Fig. 6*b*. Residue Leu^{27} in hPTHrP, which is lysine in hPTH, is included in the extensive hydrophobic interface.

hPTH and hPTHrP-(1–34) share eight identical amino acids in the region 1–13 but only three identical amino acids in the region 14–34 (Fig. 1). However, the C termini of both peptides form similar amphiphilic helices that are proposed to be responsible for high affinity receptor binding (22, 23). When residues 22–31 were substituted with a model amphiphilic sequence (ELLEKLLEKL) in the PTHrP analog RS-66271, high *in vivo* bone anabolic efficacy was demonstrated (40). CD and NMR studies confirmed that RS-66271 exists in a helical conformation from residues 16 to 32 (41). Our models for the interaction of PTH and PTHrP to the common PTH/PTHrP receptor support the hypothesis that the amphiphilic helices at the C-terminal regions of PTH and PTHrP-(1–34) are responsible for the proposed peptide-receptor recognition (22, 23).

A detailed structural analysis of PTH or PTHrP bound to its common PTH/PTHrP receptor will be required to fully understand this ligand-receptor binding and signaling. The x-ray structure of hPTH-(1–34) reported here, combined with the NMR structures and biochemical results, has allowed modeling of hPTH and hPTHrP interacting with the PTH/PTHrP receptor. This has provided a new conceptual starting point for unraveling the ligand-receptor recognition mechanism and consequently to guide structure-based design of novel PTH analogs and mimics.

Acknowledgments—We thank Drs. H. U. Bryant, J. F. Caro, W. W. Chin, R. D. DiMarchi, C. A. Frolik, M. F. Haslanger, J. M. Hock, A. H. Hunt, V. J. Klimkowski, J. Martin, B. H. Mitlak, J. D. Termine, and J.-P. Wery for helpful discussions.

REFERENCES

1. Potts, J. T., Jr., Bringhurst, F. R., Gardella, T. J., Nussbaum, S. R., Segre, G. V., and Kronenberg, H. M. (1995) *Endocrinology* **2,** 920–966
2. Sone, T., Fukunaga, M., Ono, S., and Nishiyama, T. (1995) *Miner. Electrolyte Metab.* **21,** 232–235
3. Brommage, R., Hotchkiss, C. E., Lees, C. J., Stancill, M. W., Hock, J. M., and Jerome, C. P. (1999) *J. Clin. Endocrinol. Metab.* **84,** 3757–3763
4. Lindsay, R., Nieves, J., Formica, C., Henneman, E., Woelfert, L., Shen, V., Dempster, D., and Cosman, F. (1997) *Lancet* **350,** 550–555
5. Canalis, E., Hock, J. M., and Raisz, L. G. (1994) in *The Parathyroids: Basic and Clinical Concepts* (Bilezikian, J. P., Marcus, R., and Levine, M., eds), pp. 65–82, Raven Press, Ltd., New York
6. Chase, L. R., and Aurbach, G. D. (1970) *J. Biol. Chem.* **245,** 1520–1526
7. Civitelli, R., Reid, I. R., Westbrook, S., Avioli, L. V., and Hruska, K. A. (1988) *Am. J. Physiol.* **255,** E660–E667

Downloaded from http://www.jbc.org/ by guest on November 12, 2017

8. Mosekilde, L., Sogaard, C. H., Danielsen, C. C., and Torring, O. (1991) *Endocrinology* **129,** 421–428
9. Tregear, G. W., Van Rietschoten, J., Greene, E., Keutmann, H. T., Niall, H. D., Reit, B., Parsons, J. A., and Potts, J. T., Jr. (1973) *Endocrinology* **93,** 1349–1353
10. Gardella, T. J., Axelrod, D., Rubin, D., Keutmann, H. T., Potts, J. T., Jr., Kronenberg, H. M., and Nussbaum, S. R. (1991) *J. Biol. Chem.* **266,** 13141–13146
11. Juppner, H., Schipani, E., Bringhurst, F. R., McClure, I., Keutmann, H. T., Potts, J. T., Jr., Kronenberg, H. M., Abou-Samra, A. B., Segre, G. V., and Gardella, T. J. (1994) *Endocrinology* **134,** 879–884
12. Moseley, J. M., and Gillespie, M. T. (1995) *Crit. Rev. Clin. Lab. Sci.* **32,** 299–343
13. Blind, E., Raue, F., Knappe, V., Schroth, J., and Ziegler, R. (1993) *Exp. Clin. Endocrinol.* **101,** 150–155
14. Gronwald, W., Schomburg, D., Tegge, W., and Wray, V. (1997) *Biol. Chem.* **378,** 1501–1508
15. Weidler, M., Marx, U. C., Seidel, G., Schafer, W., Hoffmann, E., Esswein, A., and Rosch, P. (1999) *FEBS Lett.* **444,** 239–244
16. Fiskin, A. M., Cohn, D. V., and Peterson, G. S. (1997) *J. Biol. Chem.* **252,** 8261–8268
17. Marx, U. C., Austermann, S., Bayer, P., Adermann, K., Ejchart, A., Sticht, H., Walter, S., Schmid, F. X., Jaenicke, R., Forssmann, W. G., and Rosch, P. (1995) *J. Biol. Chem.* **270,** 15194–15202
18. Barden, J. A., and Kemp, B. E. (1993) *Biochemistry* **32,** 7126–7132
19. Klaus, W., Dieckmann, T., Wray, V., Schomburg, D., Wingender, E., and Mayer, H. (1991) *Biochemistry* **30,** 6936–6942
20. Strickland, L. A., Bozzato, R. P., and Kronis, K. A. (1993) *Biochemistry* **32,** 6050–6057
21. Chorev, M., Behar, V., Yang, Q., Rosenblatt, M., Mammi, S., Maretto, S., Pellegrini, M., and Peggion, E. (1995) *Biopolymers* **36,** 485–495
22. Pellegrini, M., Royo, M., Rosenblatt, M., Chorev, M., and Mierke, D. (1998) *J. Biol. Chem.* **273,** 10420–10427
23. Neugebauer, W., Surewicz, W. K., Gordon, H. L., Somorjai, R. L., Sung, W., and Willick, G. E. (1992) *Biochemistry* **31,** 2056–2063
24. Otwinowski, Z., and Minor, W. (1997) *Methods Enzymol.* **276,** 307–326
25. Terwilliger, T. C., and Berendzen, J. (1999) *Acta Crystallogr. Sect. D Biol. Crystallogr.* **55,** 849–861
26. Jones, T. A., and Kjeldgaard, M. (1997) *Methods Enzymol.* **277,** 173–208
27. Brunger, A. T. (1993) *X-PLOR Version 3.1: a System for Crystallography and NMR*, Yale University Press, New Haven, CT
28. Sheldrick, G. M., and Schneider, T. R. (1997) *Methods Enzymol.* **277,** 319–343
29. Belrhali, H., Nollert, P., Royant, A., Menzel, C., Rosenbusch, J. P., Landau, E. M., and Pebay-Peyroula, E. (1999) *Structure* **7,** 909–917
30. Pellegrini, M., Bisello, A., Rosenblatt, M., Chorev, M., and Mierke, D. F. (1998) *Biochemistry* **37,** 12737–12743
31. Bisello, A., Adams, A. E., Mierke, D. F., Pellegrini, M., Rosenblatt, M., Suva, L. J., and Chorev, M. (1998) *J. Biol. Chem.* **273,** 22498–22505
32. Adams, A. E., Bisello, A., Chorev, M., Rosenblatt, M., and Suva, L. J. (1998) *Mol. Endocrinol.* **12,** 1673–1683
33. Chorev, M., Goldman, M. E., McKee, R. L., Roubini, E., Levy, J. J., Gay, C. T., Reagan, J. E., Fisher, J. E., Caporale, L. H., Golub, E. E., Caulfield, M. P., Nutt, R. F., and Rosenblatt, M. (1990) *Biochemistry* **29,** 1580–1586
34. Marx, U. C., Adermann, K., Bayer, P., Forssmann, W.-G., Roesch, P. (2000) *Biochem. Biophys. Res. Commun.* **267,** 213–220
35. Wray, V., Federau, T., Gronwald, W., Mayer, H., Schomburg, D., Tegge, W., and Wingender, E. (1994) *Biochemistry* **33,** 1684–1693
36. Mierke, D. F., Maretto, S., Schievano, E., DeLuca, D., Bisello, A., Mammi, S., Rosenblatt, M., Peggion, E., and Chorev, M. (1997) *Biochemistry* **36,** 10372–10383
37. Chorev, M., and Rosenblatt, M. (1996) in *Principles of Bone Biology* (Bilezikian, J. P., Raisz, L. G., and Rodan, G. A., eds) pp. 305–323, Academic Press, San Diego, CA
38. Rolz, C., Pellegrini, M., and Mierke, D. F. (1999) *Biochemistry* **38,** 6397–6405
39. Gardella, T. J., Wilson, A. K., Keutmann, H. T., Oberstein, R., Potts, J. T., Jr., Kronenberg, M., and Nussbaum, S. R. (1993) *Endocrinology* **132,** 2024–2030
40. Vickery, B. H., Avnur, Z., Cheng, Y., Chiou, S. S., Leaffer, D., Caulfield, J. P., Kimmel, D. B., Ho, T., and Krstenansky, J. L. (1996) *J. Bone Miner. Res.* **11,** 1943–1951
41. Pellegrini, M., Bisello, A., Rosenblatt, M., Chorev, M., and Mierke, D. F. (1997) *J. Med. Chem.* **40,** 3025–3031
42. Condon, S. M., Morize, I., Darnbrough, S., Burns, C. J., Miller, B. E., Uhl, J., Burke, K., Jariwala, N., Locke, K., Krolikowski, P. H., Kumar, N. V., and Labaudiniere, R. F. (2000) *J. Am. Chem. Soc.* **122,** 3007–3014

Downloaded from http://www.jbc.org/ by guest on November 12, 2017

Crystal Structure of Human Parathyroid Hormone 1–34 at 0.9-Å Resolution

Lei Jin, Stephen L. Briggs, Srinivasan Chandrasekhar, Nickolay Y. Chirgadze, David K. Clawson, Richard W. Schevitz, David L. Smiley, Armen H. Tashjian and Faming Zhang

J. Biol. Chem. 2000, 275:27238-27244.
originally published online August 25, 2000

Access the most updated version of this article at doi:

Alerts:
- When this article is cited
- When a correction for this article is posted

Click here to choose from all of JBC's e-mail alerts

This article cites 39 references, 5 of which can be accessed free at
http://www.jbc.org/content/275/35/27238.full.html#ref-list-1

Downloaded from http://www.jbc.org/ by guest on November 12, 2017